

## Articles

## Substituted Aluminum and Zinc Quinolates with Blue-Shifted Absorbance/Luminescence Bands: Synthesis and Spectroscopic, Photoluminescence, and Electroluminescence Characterization

T. A. Hopkins,<sup>†</sup> K. Meerholz,<sup>‡,§</sup> S. Shaheen,<sup>‡</sup> M. L. Anderson,<sup>†</sup> A. Schmidt,<sup>†,⊥</sup> B. Kippelen,<sup>‡</sup> A. B. Padias,<sup>†</sup> H. K. Hall, Jr.,<sup>\*,†</sup> N. Peyghambarian,<sup>‡</sup> and N. R. Armstrong<sup>\*,†</sup>

Department of Chemistry and Optical Sciences Center, University of Arizona, Tucson, Arizona 85721

Received July 25, 1995. Revised Manuscript Received November 20, 1995<sup>⊗</sup>

Two novel lumophores based on aluminum and zinc metallo-8-hydroxyquinolates have been prepared as electroluminescent materials, and their absorbance, photoluminescence, and electroluminescence properties compared with unsubstituted versions of these same complexes. 8-Hydroxy-5-piperidylquinolinesulfonamide (**1**) was synthesized in order to add an electron-withdrawing substituent at the 5-position in 8-hydroxyquinoline, increasing the solubility of the corresponding metal quinolate complexes in nonpolar solvents, and producing a blue-shift in the emission wavelength maximum, relative to complexes formed from the unsubstituted compound. The aluminum complex ( $\text{Al}(\text{QS})_3$ ) and the zinc complex ( $\text{Zn}(\text{QS})_2$ ) of **1** were compared with the aluminum and zinc complexes of unsubstituted 8-hydroxyquinoline ( $\text{AlQ}_3$  and  $\text{ZnQ}_2$ ), both as solutions and as pure thin films, or as poly(*N*-vinylcarbazole) (PVK) thin films doped with the metal quinolates. Ultraviolet photoelectron spectroscopy data are presented to assist in estimating the energies of the highest occupied molecular orbitals (HOMO) of  $\text{AlQ}_3$ ,  $\text{ZnQ}_2$ ,  $\text{Al}(\text{QS})_3$ , and  $\text{Zn}(\text{QS})_2$ . Electroluminescence data shows that ITO/ $\text{Al}(\text{QS})_3$ –PVK/aluminum and ITO/ $\text{Zn}(\text{QS})_2$ –PVK/aluminum devices exhibit good diode-like electrical behavior. Electroluminescence spectra mimic the photoluminescence spectra for all complexes.

### Introduction

Considerable effort is currently being expended to produce efficient electroluminescent (EL) devices that provide a variety of colors across the visible spectrum.<sup>1–6</sup> Early reports of device-quality materials employed vacuum-deposited thin films of the tris(8-hydroxyquinoline)–aluminum complex ( $\text{AlQ}_3$ ) (Figure 1) as the emitter material.<sup>1,7,8</sup> In recent years attention has been

focused on development of highly conjugated polymers such as poly(*p*-phenylenevinylene) (PPV) and related luminescent systems.<sup>6,9–12</sup> One of the goals in the design of next-generation organic LEDs is to produce polymer matrixes containing electroluminescent agents (either doped into the polymer or as part of a polymer backbone or side chain), achieving waveguide optical quality and the capability of supporting efficient charge transport.

The fluorescence properties of metalloquinolates have long been known.<sup>13</sup> While their solution fluorescence efficiencies would seem to be lower than desirable, metalloquinolate thin films are attractive candidates as EL materials. They form stable thin films, exhibit good charge transport mobilities, and have good solid-state luminescence yields.<sup>14</sup>

<sup>†</sup> Department of Chemistry.

<sup>‡</sup> Optical Sciences Center.

<sup>\*</sup> To whom correspondence should be addressed.

<sup>§</sup> Present address: Institut für Physikalische Chemie, Ludwig-Maximilian-Universität München, Sophienstrasse 11, D-80333 München, Germany.

<sup>⊥</sup> Present address: Max Planck Institute für Polymerforschung, Ackermannweg-10, Mainz, Germany.

<sup>⊗</sup> Abstract published in *Advance ACS Abstracts*, January 1, 1996.

(1) Tang, C. W.; Van Slyke, S. A. *Appl. Phys. Lett.* **1987**, *51*, 913.  
(2) Grem, G.; Leditzky, G.; Ullrich, B.; Leising, G. *Adv. Mater.* **1992**, *4*, 36.

(3) Zhang, C.; Höger, S.; Pakbaz, K.; Wudl, F.; Heeger, A. J. *J. Electron. Mater.* **1993**, *22*, 413.

(4) Braun, D.; Heeger, A. J. *Thin Solid Films* **1992**, *216*, 96.

(5) Kraft, A.; Burn, P. L.; Holmes, A. B.; Bradley, D. D. C.; Brown, A. R.; Friend, R. H.; Gymer, R. W. *Synth. Met.* **1993**, *55*, 936.

(6) Zhang, C.; Vonseggern, H.; Pakbaz, K.; Kraabel, B.; Schmidt, H. W.; Heeger, A. J. *Synth. Met.* **1994**, *62*, 35.

(7) Tang, C. W.; VanSlyke, S. A.; Chen, C. H. *J. Appl. Phys.* **1989**, *65*, 3610.

(8) Hamada, Y.; Sano, T.; Fujita, M.; Fujii, T.; Nishio, Y.; Shibata, K. *Jpn. J. Appl. Phys.* **1993**, *32*, L514.

(9) Tachelet, W.; Jacobs, S.; Ndayikenguru, H.; Geise, H. J.; Grüner, J. *J. Appl. Phys. Lett.* **1994**, *64*, 2364.

(10) Burn, P. L.; Kraft, A.; Baigent, D. R.; Bradley, D. D. C.; Brown, A. R.; Friend, R. H.; Gymer, R. W.; Holmes, A. B.; Jackson, R. W. *J. Am. Chem. Soc.* **1993**, *115*, 10117.

(11) Katz, H. E.; Bent, S. F.; Wilson, W. L.; Schilling, M. L.; Ungashe, S. B. *J. Am. Chem. Soc.* **1994**, *116*, 6631.

(12) Yang, Y.; Heeger, A. J. *Appl. Phys. Lett.* **1994**, *64*, 1245.

(13) Bhatnagar, D. C.; Forster, L. S. *Spectrochim. Acta* **1965**, *21*, 1803.

(14) Ding, H. Z.; Xing, X. S.; Zhu, H. S. *J. Physics D—Appl. Phys.* **1994**, *27*, 591.

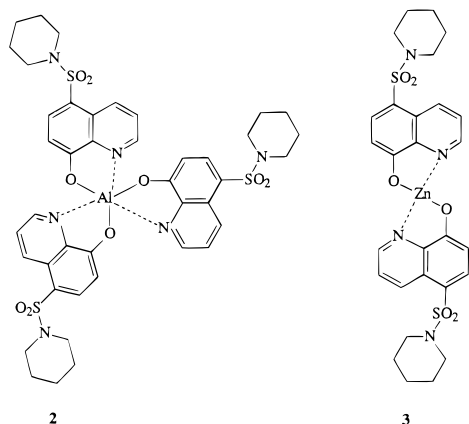
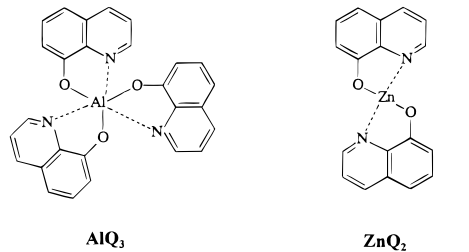


**Figure 1.** Structures of the parent complex molecules AlQ<sub>3</sub> and ZnQ<sub>2</sub> and the corresponding target complexes **2** (Al(QS)<sub>3</sub>) and **3** (Zn(QS)<sub>2</sub>) with the sulfonamide-substituted quinoline ligand.

One of the most attractive features of organic EL devices, relative to inorganic devices, is the ability to easily tune the emission wavelengths by manipulating substituents in the electroluminescent material. This has been amply demonstrated with PPV<sup>3,5,15</sup> but has hardly been explored for the metalloquinolates.<sup>8</sup> Placing electron-withdrawing substituents in the 5-position of the quinoline ring is predicted to increase the energy difference between the highest occupied molecular orbital (HOMO) and the lowest unoccupied molecular orbital (LUMO).<sup>16,17</sup> 8-hydroxy-5-quinolinesulfonate esters would appear to be one possible target with these properties, since sulfonate esters are electron-withdrawing groups that should have measureable effects on the electronic spectra. Quinolinesulfonate esters, however, are relatively rare and unstable compared to other aromatic sulfonate esters.<sup>18,19</sup> Sulfonamide substituents offer greater stability and retain the electron-withdrawing character of the sulfonate substituent.

We describe here a synthesis of 8-hydroxy-5-piperidinylquinolinesulfonamide (**1**, Figure 2), which represents a significant improvement over a previously reported synthesis of this system.<sup>20</sup> The resulting aluminum and zinc sulfonamidoquinolates **2** (Al(QS)<sub>3</sub>) and **3** (Zn(QS)<sub>2</sub>, Figure 1) exhibit blue-shifted absorbance, luminescence, and electroluminescence spectra due to the strong

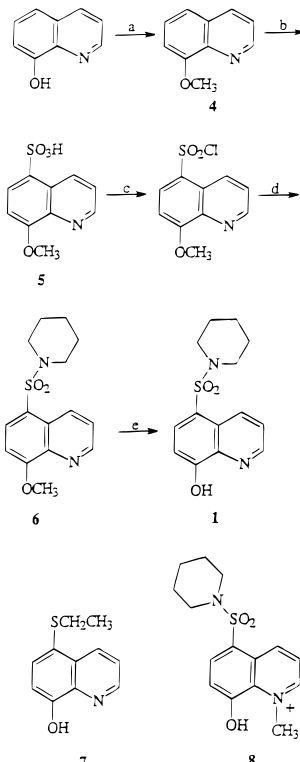


**Figure 2.** Synthetic scheme for the target ligand molecule 8-hydroxy-5-piperidinylquinolinesulfonamide **1**.

electron-withdrawing sulfonamide group, while the piperidinyl moiety increases the solubility in nonpolar solvents, compared to the unsubstituted AlQ<sub>3</sub> and ZnQ<sub>2</sub>. Preliminary electroluminescence measurements have been made by incorporating these quinolates into poly(vinylcarbazole) (PVK) thin films, to demonstrate that these new compounds should lead to device-quality materials. It is anticipated that the addition of bulky side chains to metalloquinolates should also lead to better thin film formation by impeding aggregation and crystallization, a philosophy which has guided the design of charge transport agents and polymer matrixes in recent years in multilayer electrophotographic systems.<sup>21</sup>

## Results and Discussion

**I. Synthesis.** Sulfonamide **1** was synthesized as shown in Figure 2. Details of this synthesis are discussed in the Experimental Section. 8-Hydroxyquinoline was protected as the methyl ether **4** with NaH/DMF/MeI prior to treatment with fuming sulfuric acid at 0–15 °C to give exclusively 8-methoxy-5-quinolinesulfonic acid monohydrate (**5**).<sup>22</sup> The sulfonyl chloride was obtained by heating a solution of **5** in SOCl<sub>2</sub> to reflux for 4 h in the presence of a catalytic amount of DMF. The crude sulfonyl chloride was isolated and immediately carried on to the sulfonamide by heating to reflux in CH<sub>2</sub>Cl<sub>2</sub> with excess piperidine for 4 h. Reaction times longer than 4 h for both the sulfonyl chloride and sulfonamide reactions led to lower yields of product. Flash column chromatography on silica gel afforded 8-methoxy-5-piperidinylquinolinesulfonamide (**6**).

(15) Greenham, N. C.; Moratti, S. C.; Bradley, D. D. C.; Friend, R. H.; Holmes, A. B. *Nature* **1993**, *365*, 628.  
 (16) Albright, T. A.; Burdett, J. K.; Whangbo, M.-H. *Orbital Interactions in Chemistry*; Wiley: New York, 1985.  
 (17) Coulson, C. A.; Streitwieser, A., Jr. *Dictionary of pi-Electron Calculations*; Freeman: San Francisco, 1965.  
 (18) Posner, G. H. Ph.D. Dissertation, Harvard University, 1968.  
 (19) Jpn. Kokai Tokkyo Koho JP 5877, 864; see also CA(99): P158257t.  
 (20) Yanni, A. M.; Abdel-Hafez, A. A.; Moharram, A. M. *Rev. Roum. Chim.* **1989**, *34*, 1775.

(21) Yuh, H.-J.; Pai, D. M. *Mol. Cryst. Liq. Cryst.* **1990**, *183*, 217.  
 (22) Gershon, H.; McNeil, M. W.; Grefig, A. T.; Schulman, S. G. *Anal. Chim. Acta* **1973**, *63*, 454.

Sodium thiophenoxy<sup>23</sup> was used for the demethylation of **6** since it was expected to deprotect the methyl ether without undergoing side reactions. Reaction with excess NaSPh in DMF at 60 °C demethylated **6** cleanly in quantitative yield as shown by <sup>1</sup>H NMR spectroscopy. Complete removal of thiophenol proved difficult but was ultimately accomplished by repeatedly slurring the product in hexanes/ligroin. This was accompanied by a slight loss of product. The final pale yellow sulfonamide was sublimed to give white crystals in 81% yield. The overall yield of **1** from 8-hydroxyquinoline was 54%.

Other deprotection schemes produced serious side reactions. Deprotection of **6** with sodium ethoxide in anhydrous DMF<sup>24</sup> at 60 °C cleaved the methyl ether, giving the desired product **1** along with approximately 10% of 5-(ethylthio)-8-hydroxyquinoline (**7**) as determined by <sup>1</sup>H NMR spectroscopy. *Ipsò* substitution by thioethoxide during demethylation has been noted previously in demethylation reactions of anisoles.<sup>24</sup> Deprotection of **6** was also attempted using Lewis acids such as BCl<sub>3</sub><sup>25</sup> or TMSI.<sup>26</sup> These reagents normally coordinate to the oxygen of a methyl ether, releasing halide ion. Nucleophilic attack by the halide ion demethylates the oxonium cation. However, in our case, coordination of BCl<sub>3</sub> or TMSI to the ether oxygen of **6** led to quinolinium **8** via intramolecular attack of the quinoline nitrogen on the incipient oxonium cation. Typical demethylation conditions for **8** would most likely lead to sulfonamide cleavage.

Although the synthesis of **1** has been previously reported, we found that the published method gave unreliable results.<sup>20</sup> Developing our own synthetic route, we obtained physical characterization data that differed significantly from the earlier report. Whereas our sulfonamide **1** is a white crystalline compound melting at 164–165 °C, the previous researchers reported the same sulfonamide as yellow-green crystals after recrystallization from water which melted with decomposition at a temperature of 324 °C. Notably, 8-hydroxy-5-quinolinesulfonic acid melts with decomposition at this temperature and is also a yellow powder. We believe that the authors may actually have cleaved the sulfonamide substituent during recrystallization from water, and we have seen anecdotal evidence of this ourselves. Therefore, we recommend avoiding prolonged exposure of **1** to water or alcohols.

To make the final metal quinolates we chose aluminum or zinc alkyls, which possess a large pK<sub>a</sub> difference between the basic metal ligand and 8-hydroxyquinoline. In this way, we sought to enhance the deprotonation reaction of the quinolinol and minimize any nucleophilic reactions with the substituent. AlQ<sub>3</sub> is often made from reaction of the quinoline with AlCl<sub>3</sub> or aluminum alkoxides.<sup>27–29</sup> Reaction with AlCl<sub>3</sub> generates HCl and could be a problem for acid-sensitive substituents. We

(23) Wildes, J. W.; Martin, N. H.; Pitt, C. G.; Wall, M. E. *J. Org. Chem.* **1971**, *36*, 721.

(24) Feutrill, G. I.; Mirrington, R. N. *Aust. J. Chem.* **1972**, *25*, 1719.

(25) Nagaoka, H.; Schmid, G.; Iio, H.; Kishi, Y. *Tetrahedron Lett.* **1981**, *22*, 899.

(26) Jung, M. E.; Lyster, M. A. *J. Org. Chem.* **1977**, *42*, 3761.

(27) Nakano, T.; Kato, K.; Asai, S. *Jap. Pat. JP 05279371 A2* 931026, 1995; see also *CA(120)*: 259967.

(28) Sonsale, A. Y.; Gopinathan, S.; Gopinathan, C. *Indian J. Chem., Sect. A* **1976**, *14A*(6), 408.

(29) Vevere, I.; Maijs, L.; Riekstina, D. *Latv. PSR Zinat. Akad. Vestis, Kim. Der.* **1970**, *4*, 405.

have observed that **1** is somewhat acid-sensitive, as the sulfonamide group is readily cleaved on silica gel. The aluminum alkoxides, although expected to react to give the aluminum quinolates, may also behave as nucleophiles, potentially reacting with the substituents. Treatment of **1** with stoichiometric amounts of AlEt<sub>3</sub> or ZnEt<sub>2</sub> in anhydrous THF afforded metalloquinolate **2** or **3**, respectively. The reaction is analogous to that reported by Inoue et al., in the synthesis of Al porphyrin complexes.<sup>30</sup> We are unaware of any other reported syntheses of metalloquinolates from hydroxyquinolines and metal alkyls. The reaction proceeded cleanly, immediately giving a yellow, highly fluorescent solution. Solvent removal followed by recrystallization led to **2** (91%) and **3** (75%).

Using the alkylzinc complexes to form the zinc quinolates allows the formation of the anhydrous zinc quinolate complex, which has a structure and spectroscopic properties which are different from the dihydrate complex.<sup>31</sup> <sup>1</sup>H NMR analysis of the zinc complexes, both substituted (**3**) and unsubstituted (ZnQ<sub>2</sub>), indicated two different sets of quinoline rings (1:1) in CDCl<sub>3</sub>, which collapsed to one type of quinoline ring when a stoichiometric excess of DMSO-*d*<sub>6</sub> was added. Interpretation of these results is based on the two possible structures known for the zinc quinolate complex.<sup>31</sup> The zinc quinolate complexes can exist either as the dihydrate, with water molecules occupying the axial ligand positions on the zinc atom, or as an anhydrous tetramer. The two peripheral zinc ions in the anhydrous complex are five-coordinate to the quinolate ligands, and the two central zinc ions are six-coordinate to other quinolate ligands, where a quinolate oxygen forms a bridge between two adjacent zinc ions.<sup>31a</sup> The quinolate complexes formed in this study were all created under strictly anhydrous synthesis conditions and are not expected to have sufficient water to form significant amounts of the dihydrate zinc complex. Elemental analyses and the lack of typical vibrational bands due to bound water in the IR spectra confirmed this expectation. Therefore, we conclude that the NMR spectra in CDCl<sub>3</sub> represent the tetrameric form of the anhydrous ZnQ<sub>2</sub> complexes, while DMSO is nucleophilic enough to break up the tetramers and stabilize the monomeric form by complexation to the zinc atom. The significance of this tendency to form tetrameric complexes with respect to electroluminescent device performance and the formation of new electroluminescent assemblies is under investigation.

**II. Absorption and Photoluminescence (PL).** Figure 3 shows the normalized absorption and PL spectra (with excitation at the absorption maximum) obtained from thin films of AlQ<sub>3</sub>, Al(QS)<sub>3</sub>, ZnQ<sub>2</sub>, and Zn-(QS)<sub>2</sub> as the pure compounds. We also investigated solutions in methylene chloride (not shown for clarity reasons). The maximum absorption and emission wavelengths are summarized in Table 1. As expected, the introduction of the sulfonamide substituent to the 5-position of the quinoline ring system leads to a blue-shift in the absorption and emission maxima of PVK films of Al(QS)<sub>3</sub> compared with a PVK film of the

(30) Akatsuka, M.; Aida, T.; Inoue, S. *Macromolecules* **1994**, *27*, 2820.

(31) (a) Kai, Y.; Morita, M.; Yasuoka, N.; Kasai, N. *Bull. Chem. Soc. Jpn.* **1985**, *58*, 1631. (b) Palenik, G. J. *Acta Crystallogr.* **1964**, *17*, 696.

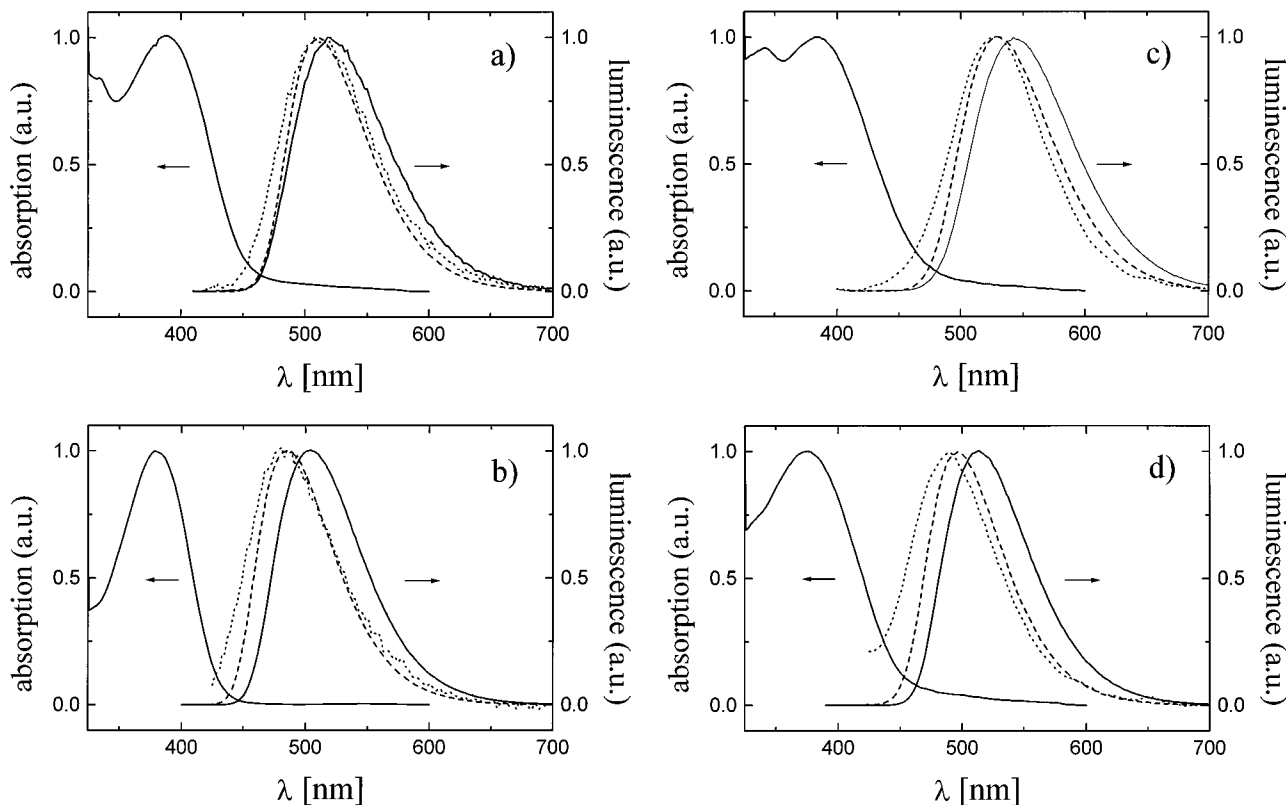


**Figure 3.** Normalized electronic spectra of (a)  $\text{AlQ}_3$ , (b)  $\text{Al}(\text{QS})_3$ , (c)  $\text{ZnQ}_2$ , and (d)  $\text{Zn}(\text{QS})_2$ : absorption and PL spectra of thin films of the pure compounds (—); PL spectra of the compounds dissolved in PVK (---); EL spectra of the devices ITO/quinolate — PVK/Al (···).

**Table 1. Absorption, Photoluminescence, and Electroluminescence Results for Solutions and Films of  $\text{AlQ}_3$ ,  $\text{Al}(\text{QS})_3$ ,  $\text{ZnQ}_2$ , and  $\text{Zn}(\text{QS})_2$**

	solution investigations			film investigations			
	abs $\lambda_{\text{max}}$ (nm)	PL $\lambda_{\text{max}}$ (nm)	Stokes shift (nm)	abs $\lambda_{\text{max}}$ (nm)	pure PL $\lambda_{\text{max}}$ (nm)	in PVK	
$\text{AlQ}_3$	390	514	126	395	519	510	508
$\text{Al}(\text{QS})_3$	379	480	101	380	502	485	482
$\text{ZnQ}_2$	379	535	161	380	542	528	530
$\text{Zn}(\text{QS})_2$	372	502	130	375	514	497	490

unsubstituted parent compound,  $\text{AlQ}_3$  (15 and 23 nm, respectively) and for PVK films of  $\text{Zn}(\text{QS})_2$  compared with those of  $\text{ZnQ}_2$ , (5 and 33 nm, respectively). Similar shifts are observed for solutions and pure metal quinolate thin films as well (see Table 1). This shift is consistent with the electron-withdrawing nature of the sulfonamide substituent. The Stokes shift is larger in the zinc complexes than for the aluminum complexes. Note that the PL spectra in solution are blue-shifted compared with those obtained from pure metal quinolate or metal quinolate/PVK thin films, while the absorption maxima remain more or less unchanged. This may be attributable to excimer formation between adjacent lumophors in the solid films, leading to a red-shift of the emission spectra. By contrast, such intermolecular processes are very much reduced in dilute solutions ( $c < 10^{-3}$  mol/L).

**III. Electroluminescence.** The two new metallo-quinolates,  $\text{Al}(\text{QS})_3$  and  $\text{Zn}(\text{QS})_2$ , decompose at elevated temperature and, therefore, cannot be vacuum sublimed. Thus, we decided to incorporate all of the quinolates into a charge-transporting polymer such as PVK, and use spin-coating techniques to fabricate first-generation LED devices, in which all of the lumophores were identically incorporated. Ideally, the resultant

luminescent layer would be bipolar (transporting both holes and electrons), allowing the recombination of charge carriers in the whole volume of the luminescent layer. Since all four compounds studied here are believed to be better electron transport than hole transport agents,<sup>1</sup> we chose a hole-conducting polymeric matrix, poly(*N*-vinylcarbazole) (PVK), for our investigations. The overall efficiencies for electroluminescence in these first doped polymer systems is quite low, but these disadvantages are offset by the fact that these electolumophore/PVK thin films do allow a systematic comparison of the electroluminescence properties of each of the metal quinolates.

The absorption maxima of the compounds in a PVK matrix are very close to those obtained in solution (Table 1), the only difference in the spectra being additional absorption originating from the carbazole units in PVK at 340 and 350 nm, respectively (not shown). The PL spectra (Figure 3) obtained from the films showed maximum luminescence at wavelengths shorter than in films of the pure compounds but longer than in solution (Table 1). This can be attributed to reduced interactions between lumophores in the PVK matrix (however, not as reduced as in solution), corresponding to reduced excimer formation. Exciplex formation, as reported/

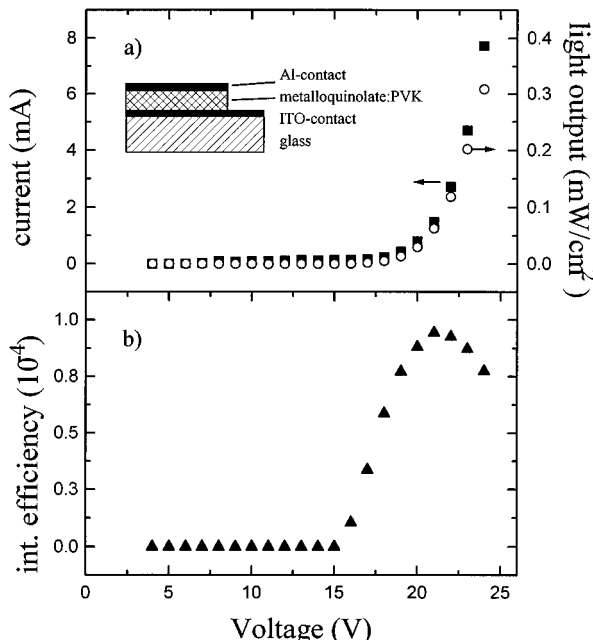


**Figure 4.** (a) Current density (■) and output light intensity (○) for the device ITO/AlQ<sub>3</sub>:PVK/Al. (b) Efficiency (output light intensity normalized to the current) (▲) of the device in (a), versus the applied voltage.

claimed by Karasz et al. for similar PVK-blends,<sup>32</sup> cannot be unambiguously excluded but seems unlikely. The shape of the spectra did not change when the excitation wavelength was varied between 300 and 450 nm (which includes the regime of strong PVK absorption). One expects to observe photoluminescence from PVK at 420 and 475 nm, respectively. The lack of these luminescent spectral features indicates that even though the photons are absorbed by the PVK, excitons at the carbazole sites can relax in energy and may be finally located on the quinolate lumophores where they eventually recombine. Similar behavior has been reported by other groups.<sup>32</sup>

Single-layer LEDs (inset, Figure 4) fabricated with the four different compounds in PVK and using ITO and aluminum as the hole and electron-injecting contacts, respectively, showed similar characteristics. We observed good diode-like behavior in the current–voltage curves. Figure 4a shows the current–voltage and the intensity–voltage curves of a device using AlQ<sub>3</sub> as the luminescent material. The turn-on voltage was 16 V. At 21 V the current density was ca. 6 mA/cm<sup>2</sup> and the light output was ca. 0.3 mW/cm<sup>2</sup> and easily visible under normal laboratory illumination. The internal efficiency was found to first increase (Figure 4b) with the applied voltage and then reach a maximum. For even higher voltages the efficiency dropped. We attribute this behavior to the heating of the sample at higher voltages (and therefore, higher currents), which may reduce the efficiency. The maximum internal efficiency was similar for devices using the four compounds as the lumophores ( $\approx 0.01\%$ ). The light output decreases exponentially over time; after 10 h of continuous operation it retains 10–15% of the original value. While this efficiency is quite low, it does demonstrate the feasibility of comparing a homologous series of electrolumophores in a polymer matrix of uniform composition. Further improvements

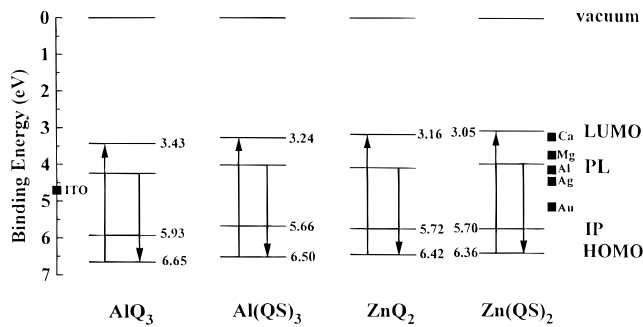


**Figure 5.** Energy (versus vacuum) of the HOMO, IP, PL, and LUMO for AlQ<sub>3</sub>, ZnQ<sub>2</sub>, Al(QS)<sub>3</sub>, and Zn(QS)<sub>2</sub> as pure thin films, prior to contact in the LED.

have been recently obtained by fabricating multilayer devices with additional transport layers for holes and electrons and will be reported elsewhere.

The EL maxima of the two aluminum compounds are identical with the PL maxima; by contrast, the EL maxima are slightly blue-shifted compared with the PL maxima for the two zinc compounds. This indicates that for the two zinc complexes an electron injection into the complex from an external source produces a slightly different “excited state” than one created by photo-excitation. A possible explanation for this might be that aluminum compounds are monomeric structures, whereas the zinc compounds are likely to exist as tetramers in the pure thin film and in the PVK matrix.<sup>31b</sup> This effect is currently under further exploration using both the monomeric (hydrous) and tetrameric (anhydrous) forms of the zinc quinolate complexes.

**IV. Ultraviolet Photoelectron Spectroscopy (UPS).** The operating voltages and efficiency of electroluminescent devices can be dependent on the barriers to charge injection into the luminescent layer, in addition to internal resistance effects. The charge injection barriers are due in part to energetic differences in the “band edge” positions of the individual organic layers comprising the device, prior to contact (e.g., the energetic difference between the work function of the cathode and the LUMO of the luminescent material). Knowledge of these band edge positions and the overall band edge picture for organic LEDs is becoming useful for development of new charge transport materials to minimize these band edge differences, and in predicting stabilities of these devices in the presence of atmospheric impurities such as oxygen.<sup>33</sup>

The absolute binding energy versus vacuum for the HOMO, the ionization potential (IP), the PL, and the LUMO levels of the four complexes are summarized in Table 2 and illustrated in the form of a band diagram in Figure 5, respectively. This figure represents the combined results of the UPS and optical experiments for the four complexes. The error in the HOMO and IP values for AlQ<sub>3</sub> and ZnQ<sub>2</sub> is  $\pm 0.15$  eV (these molecules could be vacuum deposited in UHV environments on clean metal substrates), while for Al(QS)<sub>3</sub> and Zn(QS)<sub>2</sub> the error is  $\pm 0.25$  eV due to peak-broadening in the thin films of these molecules which were cast from hexane

(33) (a) Schmidt, A.; Armstrong, N. R.; Goeltner, C.; Muellen, K. *J. Phys. Chem.* **1994**, *98*, 11780. (b) Schmidt, A.; Anderson, M. L.; Dunphy, D. R.; Wehrmeister, T.; Muellen, K.; Armstrong, N. R. *Adv. Mater.* **1995**, *7*, 772. (c) Schmidt, A.; Anderson, M. L.; Armstrong, N. R. *J. Appl. Phys.* **1995**, *78*, 5619.

**Table 2. UPS Results for the HOMO, IP, LUMO, and PL of Thin Films of AlQ<sub>3</sub>, Al(QS)<sub>3</sub>, ZnQ<sub>2</sub>, and Zn(QS)<sub>2</sub>**

	HOMO (eV)	IP (eV)	LUMO (eV)	PL state (eV)
AlQ <sub>3</sub>	6.65	5.93	<3.43	<4.26
Al(QS) <sub>3</sub>	6.50	5.66	<3.24	<4.03
ZnQ <sub>2</sub>	6.42	5.72	<3.16	<4.13
Zn(QS) <sub>2</sub>	6.36	5.70	<3.05	<3.95

solutions on freshly cleaved highly ordered graphite substrates. Values for the IP of aluminum and zinc complexes with 8-hydroxyquinoline and several 8-hydroxyquinoline derivatives have previously been reported by Hamada et al.<sup>8</sup> Our values for the IP of AlQ<sub>3</sub> and ZnQ<sub>2</sub> are in agreement, within the error of our technique (5.93 vs 5.66 eV for AlQ<sub>3</sub> and 5.72 eV vs 5.54 eV). Hamada et al. also report that the work functions of the aluminum complexes are ca. 0.1 eV farther from vacuum than those for the zinc complexes, while our results indicate that the frontier energy levels of both the zinc and aluminum compounds studied here are the same. It is anticipated that an electron-withdrawing substituent on the quinoline ring would shift the HOMO energy further from the vacuum level. Due to the uncertainty in these measurements, especially for the thin films cast on HOPG, we can only conclude at this point that the HOMO energies for all four compounds are the same within experimental error. Further investigations of this substituent effect are in progress.

As discussed previously for the AlQ<sub>3</sub> system, there is some uncertainty in estimating the LUMO position/photoluminescence state (PL) of these materials from photoelectron spectroscopy/absorbance/luminescence data alone.<sup>33</sup> There is a significant difference between the LUMO energy into which electrons are injected in an LED device, and the energetic state (PL) from which luminescence of the device actually occurs (the difference being the binding energy for the exciton, Figure 5).<sup>33</sup> Nevertheless, these measurements can be useful in establishing the upper limit for the LUMO for EL materials, which is relevant to their emission characteristics in device form. Recent electrochemical characterization of all of the metal quinolates in this paper (voltammetric measurements of the onsets for reduction and oxidation in acetonitrile) indicate that the difference between first oxidation potential and the first reduction potential is within ca. 0.1 eV of the HOMO–LUMO separation predicted by photoelectron spectroscopy/absorbance/luminescence measurements.

The energy difference between the LUMO and the work function of the negative electrode of an LED illustrates one barrier to electron injection in these devices, as shown in Figure 5, where the work functions of metals typically used as the cathode are plotted for comparison. The work function of indium tin oxide (ITO), typically used as the positive electrode in LEDs, is also plotted in Figure 4 to show the barrier to hole injection. The barrier to hole injection for all four compounds is >1 eV, while Ca, Mg, Al, or Ag can be used as the negative electrode with a barrier of 0.1–0.5 eV. These barriers can be reduced (with a corresponding decrease in device operation voltage, and an increase in device efficiency) by the appropriate choice of hole and electron transport layers.<sup>1,3–7</sup>

## Conclusions

The synthesis and characterization of two novel lumophores based on metallo-8-hydroxyquinolates has

been presented. The addition of the electron-withdrawing sulfonamide substituent to the 5-position of the quinoline ring has been shown to blue-shift the photo- and electroluminescence of aluminum and zinc complexes of 8-hydroxy-5-piperidinylquinolinesulfonamide compared to complexes with 8-hydroxyquinoline. These results indicate that molecular luminescent materials which have already demonstrated applicability in LEDs can be modified to shift their light emission and enhance their solubility in nonpolar environments, which should enhance their solubility in optical quality polymer matrices. Whether the LED efficiency of these electrolumophore thin films can be enhanced to compete with the reported efficiencies for the pure, sublimed thin films of the aluminum quinolate complex is currently under investigation. The efficiencies reported by Tang and co-workers for the vacuum deposited (ITO/hole-transport agent/Alq<sub>3</sub>/(Mg/Ag)) thin film diodes vary between 1 and 10%,<sup>1</sup> which is considerably higher than the efficiencies we observe for our first-generation thin films—the efficiencies reported here being mainly limited by charge-transfer resistance in the PVK matrix. For purposes of comparison of the two target compounds with their unsubstituted counterparts, we chose not to optimize charge transport in these thin films at this time. It is noteable, however, that the efficiencies for all four compounds were comparable, so that, using the Alq<sub>3</sub> system as a comparison, we can expect good efficiencies for substituted quinolates **2** and **3** in the next-generation thin-film devices.

## Experimental Section

**8-Methoxyquinoline (4).**<sup>34,35</sup> To a 300 mL three-neck flask fitted with magnetic stirrer, nitrogen inlet, and addition funnel was added NaH powder (3.83 g, 0.152 mol). Anhydrous DMF, 100 mL, was added, and the flask was cooled in an ice bath. A solution of 8-hydroxyquinoline (20.0 g, 0.138 mol) in 75 mL of DMF was added slowly. The reaction was stirred for 1 h at 0 °C before warming to room temperature. After H<sub>2</sub> gas evolution was complete, MeI (21.6 g, 0.152 mol) in 10 mL of DMF was slowly added. The reaction was protected from light and stirred for 2.5 h. It was then poured into 300 mL of ice water and extracted with 4 × 100 mL CH<sub>2</sub>Cl<sub>2</sub>. The combined organic layers were extracted with 100 mL of H<sub>2</sub>O followed by 100 mL of aqueous NaHSO<sub>3</sub> solution and dried over Na<sub>2</sub>SO<sub>4</sub>. Solvent was removed by rotary evaporation and the remaining residue dried in vacuo to yield **4** as a pale orange crystalline solid, 19.6 g (89%). <sup>1</sup>H NMR (250 MHz, acetone-*d*<sub>6</sub>) δ 8.85 (dd, 1H, *J* = 1.7, 4.1); 8.24 (dd, 1H, *J* = 1.7, 8.4); 7.43–7.52 (m, 3H); 7.16 (dd, 1H, *J* = 2.4, 6.5); 4.00 (s, 3H). IR (KBr) 3050, 3004, 2962, 2900, 2850, 1575, 1506, 1475, 1383, 1327, 1275, 1113, 996, 833, 800, 775, 723 cm<sup>-1</sup>. No further purification was carried out; the material was used as obtained in subsequent reactions.

**8-Methoxy-5-quinolinesulfonic Acid Monohydrate (5).** This procedure is based on the synthesis of 8-(methylthio)-5-quinoline sulfonic acid described in the literature.<sup>22</sup> In a three-neck flask equipped with magnetic stirrer and thermometer was placed 50 mL of fuming sulfuric acid (20% SO<sub>3</sub>). The flask was stoppered and cooled to 0 °C in an ice bath. Small portions of **4** (12.0 g, 75 mmol) were added carefully over a period of 3 h, keeping the temperature below 15 °C. Two 20 mL portions of fuming sulfuric acid were added when the reaction became too viscous to stir, and the reaction temperature did not change upon addition of substrate. The mixture was allowed to warm to room temperature overnight. It was then poured onto 300

(34) Aoyama, T.; Terasawa, S.; Sudo, K.; Shioiri, T. *Chem. Pharm. Bull.* **1984**, 32, 3759.

(35) Clugston, D. M.; MacLean, D. B. *Can. J. Chem.* **1966**, 44, 781.

g of crushed ice. After 5 min, a yellow precipitate was visible. The reaction was left for 20 min to ensure complete precipitation. It was then filtered, washed with ice water, and finally rinsed with acetone. The pale yellow solid was dried in vacuo to give 15.2 g (79%) of **5**. <sup>1</sup>H NMR (250 MHz, DMSO-*d*<sub>6</sub>)  $\delta$  9.81 (dd, 1H, *J* = 1.3, 8.8); 9.13 (dd, 1H, *J* = 1.3, 5.3); 8.13–8.22 (m, 2H); 7.56 (d, 1H, *J* = 8.3); 4.14 (s, 3H). <sup>13</sup>C NMR (62.9 MHz, DMSO-*d*<sub>6</sub>)  $\delta$  150.14; 145.52; 144.61; 136.79; 129.73; 127.8; 125.9; 122.9; 111.0; 57.1. IR (KBr) 3370 (br), 3098, 2933, 1609, 1557, 1490, 1387, 1310, 1250, 1200, 1145, 1050, 834, 693, 613, 600 cm<sup>-1</sup>. No further purification was attempted. The product was used as obtained in subsequent reactions.

**8-Methoxy-5-piperidinylquinolinesulfonamide (6).** In a 100 mL round-bottom flask fitted with magnetic stirrer, condenser and N<sub>2</sub> inlet were placed **5** (6.1 g, 25.5 mmol), 60 mL of SOCl<sub>2</sub>, and 1 mL of anhydrous DMF. The suspension was heated to reflux for 3 h, and complete dissolution was achieved after 30 min. After 1 h, product began to precipitate from the reaction mixture. After 3 h, the reaction mixture was cooled and transferred to a 250 mL flask before stripping off the SOCl<sub>2</sub>. The remaining SOCl<sub>2</sub> was removed by successive azeotropic distillations with CH<sub>2</sub>Cl<sub>2</sub> and toluene on a rotary evaporator. The crude sulfonyl chloride was suspended in 100 mL of CH<sub>2</sub>Cl<sub>2</sub>, and the flask was equipped with a magnetic stirrer, condenser, and N<sub>2</sub> inlet. Piperidine (15 mL) was carefully added in small aliquots, and a vigorous reaction ensued. The mixture was heated to reflux for 4 h and then cooled to room temperature. The reaction mixture was extracted with 3  $\times$  50 mL dilute aqueous acetic acid until the aqueous layer was pH 5–6. The organic layer was dried over Na<sub>2</sub>SO<sub>4</sub>. The solution was decanted and solvent removed by rotary evaporation to yield a pale orange solid. The solid was dried in vacuo to yield 8.0 g (103%) of crude sulfonamide. The crude sulfonamide was purified via flash column chromatography on silica gel. The crude material was preadsorbed onto the silica gel. The column was successively flushed with 500 mL of 1:1 EtOAc/hexanes, 500 mL of 3:1 EtOAc/hexanes, 500 mL of EtOAc, 500 mL of 30/70 MeOH/EtOAc, and finally with 1 L of MeOH. The fractions containing MeOH were collected and concentrated to yield a pale orange solid. The solid was taken up in CH<sub>2</sub>Cl<sub>2</sub> and filtered to remove silica gel. The filter was rinsed with a small amount of acetone. The solution was concentrated and the product dried in vacuo to obtain 7.3 g (94%) of **6**. <sup>1</sup>H NMR (250 MHz, CDCl<sub>3</sub> with a few drops DMSO-*d*<sub>6</sub>)  $\delta$  8.93 (dd, 1H, *J* = 1.5, 8.8); 8.87 (dd, 1H, *J* = 1.4, 4.1); 8.07 (d, 1H, *J* = 8.4); 7.47 (dd, 1H, *J* = 8.8, 4.1); 6.98 (d, 1H, *J* = 8.4); 4.03 (s, 3H); 2.96 (4H, t, *J*  $\sim$  5.3); 1.27–1.43 (m, 6H). <sup>13</sup>C NMR (62.9 MHz, CDCl<sub>3</sub> with slight DMSO-*d*<sub>6</sub>)  $\delta$  159.1; 149.4; 139.6; 133.5; 132.0, 125.6; 123.7; 122.6; 105.3; 56.3; 45.9; 24.9; 23.1. Material was used as obtained without further purification.

**8-Hydroxy-5-piperidinylquinolinesulfonamide (1).** In a 300 mL three-neck flame-dried flask fitted with magnetic stirrer, septum, and N<sub>2</sub> inlet, was placed NaH (0.556 g, 22.0 mmol) and 100 mL of anhydrous DMF. The reaction mixture was stirred under a N<sub>2</sub> atmosphere while adding PhSH, 4.0 mL, in portions. After 10 min, a clear yellow solution resulted. The solution was placed in a 60 °C oil bath. Sulfonamide **6** (1.93 g, 6.29 mmol) was added all at once. Residual **6** was rinsed in with another 50 mL of DMF. The reaction was kept at 60 °C under N<sub>2</sub> for 24 h. Water, 150 mL, was added to the reaction after 24 h, giving a cloudy solution, and the reaction flask was left in the oil bath at 60 °C for 48 h. A yellow solution with long, colorless needles resulted. The colorless crystals were filtered away from the reaction solution and treated separately. The crystals were dissolved in CH<sub>2</sub>Cl<sub>2</sub> and extracted with aqueous AcOH until the aqueous layer reached pH 5–6. The CH<sub>2</sub>Cl<sub>2</sub> layer was set aside, and the aqueous layer was extracted twice with CH<sub>2</sub>Cl<sub>2</sub>. The combined organic layers were dried over Na<sub>2</sub>SO<sub>4</sub>. The organic layer was decanted, rinsed, and stripped of solvent to give a white solid (1.30 g) smelling of PhSH. The solid was sublimed at 0.1–0.2 mmHg with mild heat (30–50 °C). White crystals were collected to yield 1.00 g and are referred to as the first crop.

The second crop of **1** was obtained from the reaction solution in the following manner. The reaction solution was extracted

with 150 mL of H<sub>2</sub>O and 2  $\times$  80 mL of hexanes. The hexanes fractions were set aside. The reaction was then extracted with 100 mL of Et<sub>2</sub>O, the ether layer was set aside. Concentrated acetic acid was added to the water layer until pH = 5 was obtained. The reaction was then extracted with CH<sub>2</sub>Cl<sub>2</sub>, 3  $\times$  100 mL. The dark green dichloromethane extracts were dried over Na<sub>2</sub>SO<sub>4</sub>. Thin layer chromatography showed the CH<sub>2</sub>Cl<sub>2</sub> layers to contain both product and PhSH.

The hexanes and ether extracts were combined with the CH<sub>2</sub>Cl<sub>2</sub> extracts of the reaction solution stripped of solvent and the residue was stirred in 10 mL of hexanes overnight. The hexanes layer was decanted off. TLC showed the hexanes contained a large amount of PhSH with some product. The residue was again stirred in 10 mL of hexanes overnight and decanted, and the residue dissolved in acetone. The acetone was removed by rotary evaporation and dried in vacuo to give 0.719 g of crude second crop. The crude material was sublimed to yield the second crop of pure **1**, 0.494 g.

The combined isolated yield of the first and second crops was 1.494 g (81%). Mp 164–165 °C; <sup>1</sup>H NMR (250 MHz, acetone-*d*<sub>6</sub>)  $\delta$  9.15 (1H, dd, *J* = 1.5, 8.8); 8.95 (1H, dd, *J* = 1.5, 4.2); 8.17 (1H, d, *J* = 8.3); 7.77 (1H, dd, *J* = 4.2, 8.8); 7.26 (1H, d, *J* = 8.3); 3.06 (4H, t, *J* = 5.4); 1.51–1.58 (4H, m); 1.38–1.50 (2H, m). <sup>13</sup>C NMR (250 MHz, CDCl<sub>3</sub>)  $\delta$  156.9; 148.0; 137.7; 133.8; 132.6; 125.1; 122.8; 121.6; 108.2; 45.8; 24.7; 23.0. Anal. Calcd for C<sub>14</sub>H<sub>16</sub>N<sub>2</sub>O<sub>3</sub>S: C, 57.52; H, 5.51; N, 9.58; S, 10.97. Found: C, 57.59; H, 5.38; N, 9.74; S, 11.11.

**Tris(5-piperidinylsulfonamide-8-quinolinolato-N<sub>1</sub>,O<sub>8</sub>)aluminum (2).** A 200 mL flask fitted with N<sub>2</sub> inlet, septum and stir bar was flame-dried and cooled under N<sub>2</sub>. Sulfonamide **1** (1.00 g, 3.42 mmol) was added along with 60 mL of anhydrous THF. Triethylaluminum (0.60 mL, 1.14 mmol) was added via syringe. A yellow solution with blue-green fluorescence was immediately visible. The reaction was stirred at room temperature for 2 days. The solution was yellow with cloudy precipitate. Solvent was stripped off and the remaining yellow residue dried in vacuo to yield 1.19 g (115%).<sup>36</sup> The solid was taken up in hot acetone, and hexanes was added until the cloud point was reached. A few drops of CH<sub>2</sub>Cl<sub>2</sub> were added until the solution was clear. The flask was cooled slowly and then stored at 0 °C for 2–3 h. Powdery yellow-green crystals were filtered off and dried in vacuo to give 0.934 g (91%) of **2**. <sup>1</sup>H NMR (250 MHz, CDCl<sub>3</sub>)  $\delta$  9.27 (1H, dd, *J* = 1.1, 8.7); 9.25 (1H, dd, *J* = 1.1, 8.6); 9.17 (1H, dd, *J* = 1.1, 8.7); 8.86 (1H, dd, *J* = 1.2, 4.8); 8.83 (1H, dd, *J* = 1.1, 4.7); 8.19 (2H, d, *J* = 8.5); 8.17 (1H, d, *J* = 8.4) 7.70 (1H, dd, *J* = 4.8, 8.7); 7.61 (1H, dd, *J* = 4.7, 8.8); 7.45 (1H, dd, *J* = 4.8, 8.8); 7.29 (1H, dd, *J* = 1.2, 4.8); 7.09 (1H, d, *J* = 8.4); 7.07 (1H, d, *J* = 8.5); 7.06 (1H, d, *J* = 8.4); 3.01–3.05 (12H, br); 1.3–1.6 (18H, m). <sup>13</sup>C NMR (62.9 MHz, CDCl<sub>3</sub>)  $\delta$  163.3; 163.1; 162.4; 145.7; 145.2; 143.3; 139.6; 139.3; 139.0; 138.9; 138.8; 136.5; 126.8; 126.7; 126.5; 123.6; 123.0; 117.4; 117.0; 116.4; 111.9; 111.6; 111.1; 46.2, 25.2; 23.4.<sup>37</sup> A sample was dried in a vacuum oven at 60 °C overnight and sent for elemental analysis. Mp 240–242 °C. IR (KBr) 3481 (br), 3089, 2936, 2843, 1608, 1567, 1506, 1455, 1400, 1384, 1336, 1250, 1217, 1157, 1092, 1033, 928, 715, 650, 553 cm<sup>-1</sup>. Anal. Calcd for C<sub>12</sub>H<sub>45</sub>AlN<sub>6</sub>O<sub>9</sub>S<sub>3</sub>: C, 55.99; H, 5.03; N, 9.33; O, 15.98; S, 10.68; Al, 2.99. Found: C, 56.05; H, 4.95; N, 9.18.

**Bis(5-piperidinylsulfonamide-8-quinolinolato-N<sub>1</sub>,O<sub>8</sub>)zinc (3).** To a 100 mL flame-dried flask fitted with N<sub>2</sub> inlet, septum, and stir bar was added sulfonamide **1** (0.494 g, 1.69 mmol) and 60 mL anhydrous THF. The flask was kept under N<sub>2</sub>. Diethylzinc (0.845 mL, 0.104 g) was added via syringe. A yellow solution with green fluorescence was visible immediately. The reaction was stirred at room temperature for 2 days. Solvent was stripped off, and the remaining yellow residue dried in vacuo to yield 0.600 g (110%).<sup>36</sup> The crude product was recrystallized from hot acetone with the addition

(36) The yield is based on **1**. The excess material was shown by <sup>1</sup>H NMR spectroscopy to be due to impurity peaks in the alkyl region originating in the metal alkyl solution.

(37) <sup>13</sup>C NMR data contains overlapping peaks that were identified and resolved by APT and DEPT experiments. A little acetone was visible in each spectrum.

of hexanes until the cloud point was reached. The filtrate was decanted off and the residue was dried in *vacuo* to give 0.55 g. <sup>1</sup>H NMR showed impurity peaks in the alkyl region from the Et<sub>2</sub>Zn solution. The product was recrystallized again from hot CH<sub>2</sub>Cl<sub>2</sub> with the addition of hexanes until the cloud point was reached. Obtained 0.44 g (75%); mp 355–357 °C. <sup>1</sup>H NMR (250 MHz, 50/50 CDCl<sub>3</sub>/DMSO-*d*<sub>6</sub>)  $\delta$  8.29 (1H, d, *J* = 8.7); 7.97 (1H, br); 7.20 (1H, d, *J* = 8.7); 6.89 (1H, dd, *J* = 4.4, 8.6); 6.07 (1H, d, *J* = 8.7); 2.18 (4H, br); 0.73 (4H, br); 0.59 (2H, br). <sup>13</sup>C NMR (62.9 MHz, 50/50 CDCl<sub>3</sub>/DMSO-*d*<sub>6</sub>)  $\delta$  144.0; 137.9; 134.9; 134.1; 125.4; 121.4; 109.0; 44.4; 22.4; 21.7. A sample was placed in a vacuum oven for 5 h at 70 °C and sent for analysis. IR (KBr): 3438, 3106, 2938, 2853, 1599, 1572, 1498, 1460, 1389, 1363, 1326, 1235, 1198, 1150, 1130, 1097, 1051, 972, 928, 838, 811, 792, 720, 621 cm<sup>-1</sup>. Anal. Calcd for C<sub>28</sub>H<sub>30</sub>N<sub>4</sub>O<sub>6</sub>S<sub>2</sub>Zn: C, 51.89; H, 4.66; N, 8.65; O, 14.81; S, 9.90; Zn, 10.09. Found: C, 52.25; H, 4.85; N, 8.40.

**Tris(8-quinolinolato-N<sub>1</sub>,O<sub>8</sub>)aluminum, AlQ<sub>3</sub>.** The parent AlQ<sub>3</sub> was synthesized using the same method as for compound **2**. Obtained 0.59 g (59%) after recrystallization; mp >400 °C. The <sup>1</sup>H NMR spectrum was consistent with an authentic sample of AlQ<sub>3</sub> supplied by Eastman Kodak. Analyses were performed on sublimed samples. IR (KBr) 3460 (br), 3050, 1605, 1579, 1500, 1469, 1385, 1330, 1115 826, 749, 649 cm<sup>-1</sup>. Anal. Calcd for C<sub>27</sub>H<sub>18</sub>N<sub>3</sub>O<sub>3</sub>Al: C, 70.59; H, 3.95; N, 9.15; O, 10.45; Al, 5.87. Found: C, 70.33; H, 4.01; N, 8.86.

**Bis(8-quinolinolato-N<sub>1</sub>,O<sub>8</sub>)zinc, ZnQ<sub>2</sub>.** The parent ZnQ<sub>2</sub> was synthesized using the same method as for compound **3**. Obtained 0.89 g (89%). A portion of the material was sublimed for analyses. Mp 367–368 °C. <sup>1</sup>H NMR (DMSO-*d*<sub>6</sub>): consistent with literature.<sup>38</sup> IR (KBr) 3440 (br), 3060, 1602, 1574, 1497, 1460, 1384, 1323, 1277, 1250, 1109, 823, 788, 734 cm<sup>-1</sup>. Anal. Calcd for C<sub>18</sub>H<sub>12</sub>N<sub>2</sub>O<sub>2</sub>Zn: C, 61.13; H, 3.42; N, 7.92; O, 9.05; Zn, 18.49. Found: C, 61.10; H, 3.53; N, 7.79.

Unless otherwise noted, all other materials were obtained from commercial suppliers and were used without further purification. Anhydrous DMF was stored over 4 Å sieves. THF was distilled from Na/benzophenone immediately prior to use. NaH was purchased as the 95 wt % powder. Triethylaluminum was obtained as a 1.9 M solution in toluene; diethylzinc as a 1.0 M solution in hexanes. For anhydrous operations, all glassware was dried prior to use and all operations were carried out under inert atmosphere.

Reported melting points (Pyrex capillary) are corrected. IR spectra were recorded with a Nicolet Impact 400D infrared spectrometer. Elemental analyses were performed at Desert Analytics in Tucson, AZ. NMR spectra were determined at 250 MHz (<sup>1</sup>H) or 62.9 MHz (<sup>13</sup>C) on Bruker FT spectrometers using TMS as the standard. Chemical shifts are reported in  $\delta$  values and are referenced to the solvent resonance peak. Coupling constants are given in hertz.

For the solution investigations the compounds were dissolved in methylene chloride (*c* = 10<sup>-3</sup>–10<sup>-4</sup> mol/L). For the solid-state investigations of the pure compounds thin films were drop-cast from methylene chloride solutions. Absorption spectra were measured with a Shimadzu U2000 spectrophotometer by using either the solutions in cuvettes of 1 mm path length or the thin films. The PL and EL spectra were recorded with a SPEX Fluorolog 1680/1681 spectrometer. The luminescence was observed from the incident surface at an angle of 30°. For the PL experiments the excitation wavelength was set at the absorption maximum of each compound, respectively.

Ultraviolet photoelectron spectroscopy (UPS) was performed using a VG ESCALAB MKII spectrometer. The occupied

electronic states were measured with HeI radiation (*h* $\nu$  = 21.2 eV). The absolute binding energy, BE<sub>vac</sub>, of the occupied states was measured versus vacuum as described in previous papers<sup>33</sup> by using a negative bias voltage (typically –5.00 V) at the sample: BE<sub>vac</sub> = *h* $\nu$  – (KE – KE<sub>onset</sub>). Here KE is the position of the photoelectron peak under investigation, and KE<sub>onset</sub> is the onset of the secondary electrons on the low kinetic energy side of the spectrum. The peak with the highest kinetic energy is caused by electrons from the HOMO level. An extrapolation of the HOMO peak down to the baseline of the spectrum was used to approximate the ionization potential (IP) of the material in the solid state. UPS of AlQ<sub>3</sub> and ZnQ<sub>2</sub> as pure thin films was carried out in *vacuo*, using procedures recently described for other electroluminescent materials and for organic materials capable of forming heterojunctions with diode-like electronic behavior.<sup>33</sup> Ultrathin films of the AlQ<sub>3</sub> and ZnQ<sub>2</sub> complexes were sublimed directly onto atomically clean Au or Ag foils, and their photoelectron spectra examined as a function of surface coverage.<sup>33</sup> The sulfonamide complexes decomposed upon sublimation, and were solution-cast from THF onto freshly cleaved highly oriented pyrolytic graphite (HOPG) surfaces for analysis.<sup>39</sup> The HOMO and IP were determined by direct comparison to the UPS data obtained from solution-cast films of the unsubstituted aluminum and zinc complexes, which had been more reliably characterized by the sublimation approach. The HOMO was clearly seen in the photoelectron spectra in all cases. The spectral features were broader for the solution-deposited samples, which increases the uncertainty in determining the binding energy of the HOMO and IP.

The LUMO level were approximated by subtracting the “optical bandgap” from the absorbance measurements (determined as the absorbance maximum with the lowest transition energy) from the HOMO binding energy.<sup>33</sup> Our approximation of the LUMO gives an upper limit for this value, because the binding energy of the photoexcited electron in the LUMO is increased by exciton formation with the remaining hole in the HOMO.<sup>33</sup>

Preliminary versions of light-emitting diodes (LEDs) were fabricated in a glovebox under nitrogen atmosphere by spin-casting solutions of the compounds (20 wt %) and PVK (80 wt %) in methylene chloride (total wt % of solids was 20 g/l) onto ITO-coated glass (resistivity <20 Ω/sq). The spin speed was 3000 rpm, resulting in film thicknesses of 100 ± 10 nm. A layer of 60 nm aluminum was evaporated as the top (electron-injecting) contact electrode. The LEDs were operated in a direct current mode in a nitrogen atmosphere. The device efficiencies were determined using a calibrated integrating sphere spectrometer (Labsphere 2000).

**Acknowledgment.** We would like to gratefully acknowledge helpful discussions with D. F. O'Brien. K.M. wishes to thank the Deutsche Forschungsgemeinschaft (Me 1246/1) for support. A.S. wishes to thank the Alexander von Humboldt Stiftung for their support (Lynen fellowship VB2-FLF). This research was supported in part by grants from the Office of Naval Research, the National Science Foundation, and the Materials Characterization Program—State of Arizona.

CM9503442

(39) (a) Ozaki, H.; Harada, Y. *J. Chem. Phys.* **1990**, *92*, 3184. (b) Harada, Y.; Ozaki, H.; Ohno, K.; Kajiwara, T. *Surf. Sci.* **1984**, *147*, 356.